ASPM and CITK regulate spindle orientation by affecting the dynamics of astral microtubules

ASPM and CITK regulate spindle orientation by affecting the dynamics of astral microtubules

Marta Gai[1*], Federico T. Bianchi[1], Cristiana Vagnoni[1], Fiammetta Vernì[2], Silvia Bonaccorsi[2], Selina Pasquero[1], Gaia E. Berto[1], Francesco Sgrò[1], Alessandra A. Chiotto[1], Laura Annaratone[3], Anna Sapino[3], Anna Bergo[4], Nicoletta Landsberger[4], Jacqueline Bond[5], Wieland B. Huttner[6] and Ferdinando Di Cunto[1*].

[1]Dept. of Molecular Biotechnology and Health Sciences, University of Turin, 10126 Turin, Italy.

[2]Dept. of Biology and Biotechnologies "C. Darwin", Sapienza, Università di Roma, 00185 Roma, Italy.

[3]Dept. of Medical Sciences, University of Turin, 10126 Turin, Italy.

[4]San Raffaele Rett Research Unit, Division of Neuroscience, San Raffaele Scientific Insitute, 20132 Milan, Italy.

[5]Leeds Institute of Biomedical and Clinical Sciences, University of Leeds, LS9 7TF Leeds, UK.

[6]Max-Planck Institute of Molecular Cell Biology and Genetics, 01307 Dresden, Germany.

* Corresponding Author. E-mail marta.gai@unito.it; ferdinando.dicunto@unito.it

Abstract

Correct orientation of cell division is considered one of the most important factors for the achievement of normal brain size, as mutations that affect this process are thought to be among the leading causes of microcephaly. Indeed, abnormal spindle orientation leads to a reduction of the neuronal progenitor symmetric divisions, premature cell cycle exit and reduced neurogenesis. This mechanism is believed to play a prominent role in microcephaly resulting from mutation of *ASPM*, the most frequently affected gene in autosomal recessive human primary microcephaly (MCPH), but it is presently unknown how ASPM regulates spindle orientation.

In this report, we show that ASPM may play this role through the interaction with Citron-kinase (CITK), whose inactivation leads to a severe form of microcephaly in mammals. Indeed, we demonstrate that CITK plays a phylogenetically conserved role in regulating spindle orientation. Moreover, ASPM is required to recruit CITK at the centrosome and CITK overexpression rescues ASPM phenotype. Finally, both ASPM and CITK loss alter the organization of astral MT and CITK regulates both astral MT nucleation and stability.

Introduction

The orientation of cell division must be carefully controlled in both embryonic and adult tissues in order to regulate cell fate, generate tissue shape and maintain tissue architecture (Bergstralh and St Johnston, 2014; Noatynska et al., 2012; Panousopoulou and Green, 2014). Studies conducted over the last two decades have established that this process is crucial to regulate the delicate balance between proliferation and differentiation that underlies normal brain development, with particular regard to the generation of the normal number of cortical neurons (Noatynska et al., 2012; Peyre and Morin, 2012; Taverna et al., 2014). During embryogenesis, the cerebral cortex is first composed of a single layer of neuroepithelial (NE) cells, which initially expand through symmetric divisions (Arai et al., 2011; Fietz and Huttner, 2011; Morin and Bellaiche, 2011; Paridaen and Huttner, 2014). As development progresses, NE progenitors give rise to radial glia (RG) cells that may further expand by dividing symmetrically or may switch to asymmetric division, producing a self-renewing progenitor and a daughter cell committed to differentiation (Calegari and Huttner, 2003; Florio and Huttner, 2014; Noctor et al., 2004; Taverna et al., 2014). A key feature of proliferative divisions of NE and RG cells is that cleavage occurs perpendicular to the ventricular surface of the neuroepithelium, while the switch from symmetric to asymmetric divisions is accompanied by a deviation of the cleavage plane (Chenn and McConnell, 1995; Kosodo et al., 2004; Lancaster and Knoblich, 2012). Oriented cell division is achieved through the proper positioning of the mitotic spindle (Castanon and Gonzalez-Gaitan, 2011; Gillies and Cabernard, 2011; Williams and Fuchs, 2013), which depends on the formation of molecular links between the actin-rich cell cortex and the astral MT emanating from the centrosome-derived spindle poles (Busson et al., 1998; Lancaster and Knoblich, 2012; Samora et al., 2011). Indeed either loss of Doublecortin (*DCX*), which destabilizes MT (Pramparo et al., 2010), or mutations of *LIS1*, *NDE1* and *NDEL1*, which disrupt dynein–dynactin function at the cell

cortex (Feng and Walsh, 2004; Schwamborn and Knoblich, 2008; Yingling et al., 2008), randomize the mitotic spindle in NE progenitors and lead to their early exhaustion. A similar depletion of progenitor cells, correlated to randomized spindle orientation, can be produced by disruption of proteins involved in centrosome function (Fish et al., 2006; Gruber et al., 2011; Megraw et al., 2011; Thornton and Woods, 2009). Accordingly, mutation of many proteins contributing to centriole biogenesis, centrosome maturation and spindle organization (Bettencourt-Dias et al., 2011; Loffler et al., 2011) has been strongly associated to human primary microcephaly (MCPH). MCPH is characterized by a reduced head circumference accompanied by a relatively preserved brain architecture, resulting in mild to moderate intellectual disability and few associated symptoms (Kaindl et al., 2010; Mochida, 2009). Thirteen MCPH loci (MCPH1-MCPH13) have been mapped to date (Faheem et al., 2015; Sir et al., 2011) and it has been established that most of the encoded proteins are capable of localizing at the centrosome, at the spindle poles or at the spindle. Nevertheless, our understanding of how these proteins may affect spindle orientation and cell fate determination is still very limited. *ASPM* (abnormal spindle-like microcephaly associated, *MCPH5*) is the most frequently mutated gene in MCPH (Bond et al., 2002; Thornton and Woods, 2009). ASPM is a conserved protein that associates with the MT minus ends, is recruited at the spindle poles during mitosis and controls spindle MT organization, spindle function and cytokinesis from insects to mammals (Higgins et al., 2010; Wakefield et al., 2001). In mammals, NE cells with reduced ASPM expression fail to orient the mitotic spindle perpendicular to the ventricular surface of the neuroepithelium and show an increased frequency of asymmetric divisions, therefore reducing the pool of neuronal precursors (Fish et al., 2006; Pulvers et al., 2010). However, it is presently unknown how ASPM regulates spindle orientation. Previous studies (Paramasivam et al., 2007) showed that ASPM physically interacts with Citron Kinase (CITK), a protein involved in control of cytokinesis (Di Cunto et al., 2000; Madaule et al., 1998), whose inactivation in

rodents results in dramatic microcephaly and lethal epilepsy (Di Cunto et al., 2000; Sarkisian et al., 2002).

In this report we show that, in addition to its role in cytokinesis, CITK plays a phylogenetically conserved role in the control of mitotic spindle orientation, by promoting the nucleation and stabilization of astral MT. Moreover, we show that CITK is recruited to the spindle by ASPM and that CITK overexpression may rescue the spindle orientation defect elicited by ASPM knockdown. Altogether, our results provide new insight into the mechanisms by which ASPM loss may cause microcephaly and suggest that a spindle orientation defect may contribute to the CITK microcephaly phenotype.

Results

1. CITK is a phylogenetically conserved determinant of spindle orientation.

On the basis of a previous report showing that CITK may physically interact with ASPM (Paramasivam et al., 2007) and of the prominent role played by ASPM in regulating spindle orientation (Fish et al., 2006; Higgins et al., 2010), we asked whether, besides controlling abscission (Gai et al., 2011), CITK also plays a role in spindle orientation. To address this question, we first examined whether it contributes to maintaining the mitotic spindle positioned perpendicular to the apical–basal axis of mouse NE progenitors. To do so, we immunostained fixed cryosection of E14.5 mice neocortices for the spindle pole protein γ-tubulin and for DNA and we measured the angle formed by the cleavage plan of anaphase or telophase apical NE progenitors with the apical surface of the cortex (Chenn and McConnell, 1995; Fish et al., 2006; Konno et al., 2008; Kosodo et al., 2004) (Fig. 1A). Cell division angle was defined as vertical when it was comprised between 75° and 90° and oblique when it was in the range from 0 to 75°. Most of the apical progenitors (75%) divide vertically in CITK +/+ cortices, while only 24% of cells in the cerebral cortex of CITK -/- mice divided with vertical cleavage planes (Fig. 1B), indicating that spindle orientation is perturbed by CITK loss.

To evaluate whether this phenotype may be correlated with an increased commitment of progenitors to differentiation, we pulse-labeled E14.5 embryos with BrdU and analyzed how many cells have left the cell cycle 24 hours later, by quantifying the percentage of BrdU-positive cells which had become negative for the cell cycle marker Ki67 (Calegari et al., 2005). Interestingly, this analysis revealed a significant increase of the percentage of BrdU-positive/Ki67-negative cells both in the apical region and in the intermediate zone (Fig. 1C), strongly suggesting that altered spindle orientation is accompanied by pre-mature exit from cell cycle in CIT-K -/- developing cortices.

Since the sequence of CITK is very well conserved between *Drosophila* and mammals, and since the loss of CITK in *Drosophila* produces a cytokinesis-failure phenotype remarkably similar to the phenotype detected in mammalian cells (D'Avino et al., 2004; Echard et al., 2004; Naim et al., 2004; Shandala et al., 2004), we asked whether the role of CITK in spindle orientation is conserved as well. To address this question, we analyzed neuroblast (NB) divisions in larval brains from individuals homozygous for either dck^{1} or dck^{2}, two presumptive null alleles at the locus encoding the *Drosophila* orthologue of CITK (Naim et al., 2004). *Drosophila* NB are stem cells that divide asymmetrically, to give rise to another NB and to a smaller ganglion mother cell (GMC) committed to differentiation. To ensure a correct asymmetric division, NB spindle must be aligned to the cell polarity axis determined by the differential apico-basal concentration of several proteins. The basal cortex is enriched in proteins that are preferentially segregated into the GMC at the end of division and whose localization is in turn mediated by a large multiprotein complex that concentrates at the apical cortex (Homem and Knoblich, 2012). We immunostained wild type and *dck* mutant larval brains for Tubulin and for the basal marker Miranda (Mira) and measured the angle between a line connecting the two spindle poles and a line bisecting the crescent formed by Mira in metaphase NBs (Fig. 1D). The angle ranged between 0° and 5° in 88% of control NBs (Fig. 1E), indicating a tight coupling of the mitotic spindle with

the polarity axis. Conversely, although both *dck1* and *dck2* mutant NBs consistently displayed a well formed Mira crescent, the majority of the spindles showed more oblique orientations, ranging from 6° to 45° (n= 33 for *dck1*, and 45 for *dck2*, respectively; Fig. 1E). These results indicate that, besides to its role in abscission control, CITK plays a phylogenetically conserved role earlier in mitosis, to ensure correct positioning of the mitotic spindle.

To better characterize this function, we resorted to HeLa cells, which are sensitive to CITK depletion and have been extensively used to study spindle positioning mechanisms (Matsumura et al., 2012). We depleted CITK in these cells by RNAi using a validated sequence (Gai et al., 2011) (Fig. S1A), and analyzed cell division through phase-contrast time-lapse microscopy. Interestingly, while almost 100% of the cells treated with control siRNA divided with a cleavage plan perpendicular to the plan of the culture dish (vertical division, Fig.1G), 23.7% of the cells treated with CITK-specific siRNAs divided along an oblique plan (oblique division, Fig.1G), with one of the daughters going out of the focal plan during observation (Fig. 1F-H and Movies 1 and 2). We then analyzed, in fixed samples, the angles formed by metaphase spindles with the culture dish. CITK-depleted cells displayed a distribution of the angles skewed towards high values and a significant increase in the angle average (Fig. 1I-J). A similar phenotype was observed by inducing CITK depletion with a second, independent siRNA sequence (Fig. S1B). The phenotype was rescued by restoring CITK levels through the expression of an RNAi-resistant construct, further confirming that it is due to CITK depletion rather than to off-target effects of the siRNA sequences used (Fig. S1C).

Altogether, these results indicate that CITK is a conserved determinant of spindle orientation and demonstrate that it acts in mitosis even before its enrichment at the cleavage furrow and midbody during cytokinesis.

2. CITK is associated with mitotic spindle poles through ASPM.

Although several proteomic studies reported the association of CIT-K with the mitotic spindle (Malik et al., 2009; Nousiainen et al., 2006; Sauer et al., 2005), this localization has not been further confirmed using other techniques. Previous immuno-localization studies have shown that CITK is localized to the nucleus in interphase cells, accumulates in the cytoplasm before anaphase and becomes enriched at the cleavage furrow and at the midbody during cytokinesis (Liu et al., 2003; Madaule et al., 1998). A similar pattern was detected by live cell imaging in HeLa cells expressing physiological levels of GFP-tagged CITK from a stably integrated BAC transgene (Hutchins et al., 2010; Maliga et al., 2013; Neumann et al., 2010) (Movie 3). As expected, during mitosis, the protein appears to be evenly distributed in the cytoplasm and no enrichment is visible at the spindle or at the cell cortex (Movie 3).

Although these data confirmed the previous reports (Liu et al., 2003; Madaule et al., 1998), they did not exclude the possibility, raised by proteomic studies (Malik et al., 2009; Nousiainen et al., 2006; Sauer et al., 2005), that a pool of the protein may associate with the mitotic spindle. To address this issue, we performed a mild detergent extraction before fixation, which removes cytosolic proteins and facilitates the visualization of cytoskeleton-associated proteins. Under these conditions, immunofluorescence with anti-CITK antibodies detected a clear enrichment of the protein on both the spindle and the spindle poles, which partially overlapped with the γ-tubulin signal (Fig. 2A). This signal disappears in cell treated with CITK siRNA (Fig. 2A). Similar results were obtained using anti-GFP antibodies in HeLa cells expressing GFP-tagged CITK from a BAC transgene (Neumann et al., 2010) (Fig. 2B). A specific association of CITK with spindle poles was further validated through biochemistry, as we found that CITK is enriched in centrosomal preparations obtained from HeLa cells synchronized in metaphase (Fig. 2C). In addition, we observed that the signals of both CITK endogenous protein and CITK-GFP extensively overlap with the ASPM immunoreactivity at the spindle poles (Fig. 2D-E).

To further confirm the physical interaction between CIT-K and ASPM, we performed an *in situ* proximity ligation assay (PLA) which can reveal if two proteins are at a distance <40 nm (Soderberg et al., 2006). In mitotic cells expressing ASPM-GFP and immunostained for GFP and CITK, we observed a specific signal both within the cytoplasm and on the spindle (Fig. 2F), whereas no signal was detected in normal HeLa cells treated in the same way. This result, together with the prominent association of ASPM with the spindle poles, suggests that ASPM may be required for CITK recruitment to the spindle. We therefore analyzed the localization of CITK in ASPM-depleted cells and vice versa. While the localization pattern of ASPM was not affected by CITK-RNAi (Fig. 2G), we found that the number of cells positive for CITK at the spindle poles was significantly decreased in ASPM-depleted cells (Fig. 2H), indicating that CITK could act downstream of ASPM.

3. CITK regulates astral MT organization downstream of ASPM.

Proper orientation of mitotic spindle during mitosis requires a dynamic connection of astral MT to the cortical cytoskeleton through the MT motor complex Dynein/Dynactin, which is localized at a cortical crescent by cortical adaptor proteins such as NuMA (Busson et al., 1998; Carminati and Stearns, 1997; Nguyen-Ngoc et al., 2007; Yang et al., 2014). We therefore analyzed by immunofluorescence whether CITK absence alters the localization of these proteins at metaphase. No significant changes were observed in the localization pattern of Dynein or NuMA (Fig. S2A-C), while the percentage of cells with a Dynactin (P150) crescent was increased (Fig. S2A-C), indicating that the phenotype induced by CITK depletion cannot be explained by defective localization of these proteins. Moreover, no differences were observed in the fluorescence intensity of these proteins at spindle poles (Fig.S2A-C).

In contrast, if compared to controls, CITK-depleted cells displayed a significant reduction in the number and in the length of astral MT (Fig. 3A-B); a similar phenotype was observed in the case of ASPM depletion (Fig. 3A-B). These data indicate that CITK and ASPM may act

through similar mechanisms, impinging on the organization of astral MT. To test the possibility that an increase in CITK expression may compensate for ASPM loss, we transfected ASPM-depleted cells with CITK overexpression constructs. Remarkably, the overexpression of CITK reverted the reduction of astral MT (Fig. 3C) and the average increase of mitotic angle (Fig. 3D) elicited by ASPM depletion back to control values. In contrast, these effects where not observed when ASPM-depleted cells were cotransfected with a kinase-dead mutant of CITK (CKD) or with CITN (Fig. 3D), a brain-specific isoform of CITK completely lacking the kinase domain (Furuyashiki et al., 1999).

To functionally assess whether the spindle-orientation phenotype elicited by CITK or ASPM knockdown depends on MT stability, we treated HeLa cells, depleted for either proteins, with low doses of the MT-stabilizing drug Paclitaxel, which are known to specifically affect the most dynamic pool of MT (Mora-Bermudez et al., 2014). In both cases, the average of mitotic spindle angles was restored to control values (Fig. 3E).

4. CITK regulates astral MT length, stability and nucleation.

To investigate which aspects of the dynamic behavior of MT are affected by CITK, we performed RNAi in HeLa cells stably expressing the +TIP protein EB3, fused with the fluorescent Tomato tag, to track the plus ends of growing MT by time lapse fluorescence microscopy (Samora et al., 2011) (Fig4A). Quantitative analysis of the corresponding movies allows the estimation of different dynamic parameters, as has been previously described (Samora et al., 2011; Wandke et al., 2012) (Fig. 4B). This technique revealed that CITK loss leads to decreased MT stability and maximal distance travelled from the spindle pole towards the cell cortex, while no differences were observed in MT growth speed (Fig. 4C). Moreover, we observed a decrease of nucleation frequency (Fig. 4C).

To better address the latter phenotype we resorted to MT growth assay after cold-induced depolymerization, induced by incubating cells at 4°C for 30 minutes. 10 minutes after switching from 4°C to 37°C, the number of cells showing detectable MT growth (aster size

>1μm) was significantly decreased in CITK-depleted cells (Fig. 4D-E). Moreover, although at 15 minutes the value of this parameter was comparable to the control, the aster size was still significantly smaller in CITK-depleted cells (Fig. 4E). Altogether, these results indicate that CITK loss decreases MT nucleation and MT stability in mitotic cells.

Discussion

We here provide evidence that the previously described physical interaction between the microcephaly proteins CITK and ASPM plays a functional role in determining mitotic spindle orientation, through the regulation of astral MT dynamics. ASPM and its orthologue proteins in invertebrates have long been associated with the organization of mitotic spindle MT. Indeed, these proteins are tightly bound to the MT minus ends and are associated with the pericentriolar matrix of spindle poles (Higgins et al., 2010; Saunders et al., 1997; Wakefield et al., 2001). In *Drosophila*, the loss of *asp* prevents the focusing of MT minus ends at the spindle poles and disrupts the organization of astral and central spindle MT. These alterations lead to a semi-lethal phenotype, in which cells possessing a very active spindle integrity checkpoint arrest at metaphase while cells with a weaker spindle integrity checkpoint can progress to anaphase, but frequently fail cytokinesis (Wakefield et al., 2001). In mammals, and especially in humans, the phenotype produced by truncating mutations of ASPM is predominantly characterized by microcephaly (Bond et al., 2002; Pulvers et al., 2010). Moreover, ASPM depletion by RNAi in neuroepithelial cells reduces the ratio of symmetric, self-renewing divisions (Fish et al., 2006). Accordingly, spindle misorientation has been observed in ASPM-depleted cultured cell lines (Higgins et al., 2010), which show in addition a cytokinesis-failure phenotype (Higgins et al., 2010). On this basis, the current view is that ASPM loss of function produces microcephaly in humans principally by altering mitotic spindle orientation, thereby reducing the expansion of NE progenitors (Kaindl et al., 2010). However, since ASPM is mainly associated with the spindle poles (Fish et al., 2006; Higgins et al., 2010; Pulvers et al., 2010), how it could

affect spindle positioning remained an open question. On the other hand, it has been demonstrated that the loss of CITK in rodents produces a microcephaly phenotype much stronger than the phenotype produced by ASPM truncation (Di Cunto et al., 2000; Sarkisian et al., 2002). This is believed to result primarily as a consequence of apoptosis, secondary to cytokinesis failure, although it was shown that CITK could also be involved in the metaphase to anaphase progression (LoTurco et al., 2003). Indeed, CITK is prominently localized at the cleavage furrow and at the midbody of mitotic cells (Madaule et al., 1998) and both its genetic inactivation and its RNAi-mediated depletion result in cytokinesis failure at the abscission stage (Bassi et al., 2011; Gai et al., 2011). Therefore, although the two proteins are associated to microcephaly and were found to form a complex in HeLa cells and in developing neural tissue (Paramasivam et al., 2007), it remained unclear whether their interaction could have any relevance for microcephaly. The fact that a pool of ASPM colocalizes with CITK at the midbody (Paramasivam et al., 2007) and that ASPM-depleted cells display cytokinesis failure (Higgins et al., 2010) raised the possibility that the two proteins could functionally interact to ensure cytokinesis completion, and that abnormal cytokinesis and apoptosis could contribute to ASPM-mediated microcephaly. However, a significant increase of the latter events has not been documented in vivo neither in humans nor in mouse. Our results provide new insight on these issues. Indeed, we have shown that, in addition to its well documented role in cytokinesis, CITK is functionally implicated in the control of spindle orientation. This conclusion is based on the phenotypes observed in CITK-depleted HeLa cells, in the developing neocortex of CITK-knockout mice and also in two different *Drosophila* mutant lines, underscoring the physiological and phylogenetic relevance of this function. On this basis, it is therefore possible that the microcephaly produced in mammals by CITK loss is not only due to cytokinesis failure and apoptosis, but also to a reduced expansion of the cortical neural stem cells pool. The previous observation that CITK mutant rats display a

dramatic reduction of adult neural stem cells (Ackman et al., 2007) and the increased exit from cell cycle of proliferating progenitors which we have detected (Fig. 1C-D) are consistent with this view. However, we cannot completely exclude the possibility that these abnormalities are a secondary effect of the cytokinesis failure phenotype and deeper studies will be required to assess the relative contribution to microcephaly of the two phenotypes. Nevertheless, the implication of CITK in spindle orientation allowed us to evaluate the interaction between CITK and ASPM in a new perspective. Indeed, we found that the two proteins are tightly co-localized not only at the midbody during cytokinesis, but also at earlier mitotic stages. A pool of CITK is indeed stably associated with the spindle and the spindle poles during metaphase. Remarkably, this localization is dependent on ASPM, while the localization of ASPM is not dependent on CITK. Even more importantly, both CITK and ASPM knockdown do not disturb the localization of the proteins required to anchor astral MT to the membrane, but significantly alter the organization of astral MT. We also demonstrated that MT stability is crucial for the spindle orientation phenotypes elicited by depletion of both proteins, as they are rescued by low doses of MT-stabilizing agent. Our observations strongly suggest that ASPM and CITK regulate spindle orientation primarily by affecting the dynamics of astral MT. In this function, CITK is most likely a downstream mediator of ASPM, because its recruitment to the spindle is ASPM-dependent, while CITK knockdown does not affect ASPM localization, and because the overexpression of CITK can rescue the effects of ASPM knockdown. Therefore, we propose that ASPM promotes the correct organization of astral MT by recruiting CITK to them, thus allowing the anchorage of the spindle to the cell cortex required for a proper orientation. But how may CITK modulate astral MT organization? The analysis of MT dynamics in CITK-depleted cells revealed that the reduction of astral MT is caused by a combination of decreased nucleation and decreased stability. Moreover, the kinase activity of CITK is essential for this function, since the expression of mutants completely lacking

the kinase domain or mutated in the ATP-binding pocket do not rescue the spindle orientation phenotype. The function of CITK in cytokinesis has already been linked to MT organization. For instance, it has been proposed that CITK promotes midbody maturation by recruiting at the midbody the kinesins KIF14 (Bassi et al., 2013; Gruneberg et al., 2006) and MLKP1 (Bassi et al., 2013), which in turn recruit the MT-crosslinking protein PRC1. In addition, systematic proteomic studies have found that CIT-K may also interact with the kinesin KIF4a and KIF10 (Maliga et al., 2013). However, the roles of these proteins in MT nucleation and stabilization, in astral MT organization and in spindle orientation have not been so far investigated. Addressing the functional significance of CITK interaction with these proteins and identifying the substrates of CITK in spindle orientation control will be an interesting subject for future studies. In addition, it will be very interesting to address whether other MCPH proteins associated with MT function, such as WDR62, CDK5RAP2, CENPJ and STIL (Kaindl et al., 2010) may regulate astral MT functionally cooperating with ASPM and CITK.

Material and Methods

Cell culture, synchronization and drug treatments

HeLa cells were cultured in RPMI medium supplemented with 10% fetal bovine serum (FBS) and 1% penicillin/streptomycin. HeLa cells expressing GFP-tagged CITK and ASPM from a BAC transgene were obtained by courtesy of Hyman Lab (Max Planck Institute of Molecular Cell Biology and Genetics, Dresden) cultured in DMEM 10% heat inactivated FBS, 1% penicillin/streptomycin, 0.4 mg/ml G418, Geneticin® (Life Technologies). The HeLa cell line expressing EB3–tdTomato (Straube and Merdes, 2007), obtained by courtesy of Dr. Ann Straube (University of Warwick, Coventry, United Kingdom) was maintained in DMEM-GlutaMAX (Invitrogen) supplemented with 10% FBS, 100 Uml^{-1} penicillin, 100μgml^{-1} streptomycin, 200μgml^{-1} Geneticin (Sigma) and 0.5μgml^{-1}

puromycin (Samora et al., 2011). All cells were cultured in a humidified 5% CO2 incubator at 37°C.

Cells were synchronized by a double- or single-thymidine block. For the double thymidine block, asynchronous cultures were treated with 2 mM thymidine (Sigma) for 16 h, then released for 4–6 h in fresh complete medium and again blocked for 16 h. Finally, cells were washed twice with fresh medium and allowed to progress through mitosis.

For drug treatments, synchronized HeLa cells were treated with 250 pM of Paclitaxel (Sigma) for 30 minutes before fixation for immunofluorescence.

Transfection, RNAi and rescue

In this study, we used a previously validated (CK1 = AUGGAAGGCACU AUUUCUCAA) (Gai et al., 2011) and a second CITK-siRNA sequence (CK2 = CCAUUCCUUGGCACCUGCUU). The knockdown of ASPM was obtained using a previously validated sequence (Higgins et al., 2010) (GUGGUGAAGGUGACCUUUC). All siRNAs were obtained from GE-Healthcare (Dharmacon, Lafayette, CO). The ON-TARGETplus non-targeting siRNA #1 (GE Healthcare, Dharmacon) was used as a negative control for potential off-target effects. The expression construct coding for CITK-Cherry was generated by inserting the Myc-CITK cDNA into the pm-Cherry-N1 plasmid (Clontech, Mountain View, CA) (Gai et al., 2011). The same method was used to generate constructs coding for CKD-Cherry and for CITN-Cherry. HeLa cells plated on a six-well plate were transfected using 1 µg of the required plasmid DNA and 3 µl of *Trans*-IT-LT1 transfection reagent (Mirus Bio, Madison, WI), or 6.25 µl of the required siRNA (20 µM) and 2.5 µl Lipofectamine 2000 (Invitrogen, Carlsbad, CA), according to the manufacturers' instructions. For rescue experiments, cells were transiently transfected with siRNAs; 24 h later cells were transfected with DNA constructs and analyzed 24 h later.

Cell staining

Fixation methods are as follows: for α-tubulin staining, 4% paraformaldehyde at room temperature for 10 min or with methanol at -20°C for 10 min; for γ-tubulin, ASPM and NuMA staining, methanol at -20°C for 10 min; for Dynactin, Dynein staining, cells were pre-extracted in 0.5% Triton X-100 in PHEM buffer (60 mM PIPES, 25 mM HEPES, 10 mM EGTA, and 4 mM MgSO4) for 1 min, and then fixed in methanol at -20°C for 10 min; for CITK staining, cells were pre-extracted in 0.5% Triton X-100 in PHEM buffer for 1 min and fixed with 4% paraformaldehyde at room temperature for 10 min. In all cases, cells were permeabilized in 0,1% Triton X 100 in PBS for 10 minutes, saturated in 5% BSA in PBS for 30 minutes and incubated with primary antibody for 45 min at room temperature. Primary antibodies were detected with anti–rabbit Alexa Fluor 488 or 568 (Molecular Probes, Invitrogen), anti–mouse Alexa Fluor 488 or 568 (Molecular Probes, Invitrogen) used at 1:1000 dilution for 30 min. Counterstaining was performed with the DNA dye DAPI (Sigma) at 0.5 µg/ml for 1 minute.

The following primary antibodies were used: mouse anti-α-tubulin (1:1000 Sigma), rabbit anti-α-tubulin (1:200 Abcam), mouse anti-γ-tubulin (1:200 Abcam), rabbit anti-γ-tubulin (1:1000 Abcam), mouse anti-CITK (1:100 BDTransLab), rabbit anti-Numa (1:2000 Abcam), rabbit anti-Dynein Heavy Chain (1:300 Santa Cruz), rabbit anti-ASPM (1:2000 (Higgins et al., 2010)), mouse anti-p150 (1:1000 BDTransLab), rabbit anti-GFP (1:1000 Abcam).

Mouse embryonic cortex staining

Embryonic brains were dissected at E14.5 and fixed for 12-16h at 4°C in 4% PFA. For cell cycle exit analysis, pregnant females were previously injected at E13.5 with 75 mg/kg BrdU. Fixed brains were equilibrated in 30% sucrose in PBS for 12-24h at 4°C. Brains were embedded with Tissue-TEK (O.C.T, Sakura Finetek), snap frozen in liquid nitrogen and stored at -20°C. Sectioning was performed at 20µm with a cryostat. Cryosections were rehydrated five times in PBS before further processing. For measurement of spindle

angle, cryosections were subjected to antigen retrieval by heating in 0.01 M citrate buffer pH 6.0 at 70°C for 1 h. Sections were then permeabilized using 0.3% Triton X-100 in PBS for 30 min and quenched with 0.1 M glycine for 30 min. Sections were then incubated with anti γ-tubulin primary antibody overnight at 4°C, followed by secondary antibody for 1 h at room temperature in a solution of 0.2% gelatin, 300 mM NaCl, and 0.3% Triton X-100 in PBS. DNA was stained in the last wash using DAPI. For cell cycle exit experiments, BrdU antigen was retrieved using 2N HCl and a 10 min in a steamer, followed by neutralization with 0.1M borate buffer pH 8.5. Slides were then processed for IF using anti-Ki67 and anti-BrdU antibodies as described above for γ-tubulin.

***Drosophila* strains**

The *Drosophila citron kinase*^{1} *(ck*^{1}*)* mutant allele, also called *l(3)7m-62* or *sticky*^{1} *(sti*^{1}*)*, is described by Gatti and Baker (1989) and by FlyBase (http://flybase.bio.indiana.edu/).

The *dck*^{2} allele was isolated from a collection of 1600 ethylmethanesulfonate (EMS)-induced third chromosome late lethals, generated in Charles Zuker's laboratory (University of California, San Diego, CA) (Naim et al., 2004). *ck*^{1} and *ck*^{2} mutants alleles were kept in stocks over the TM6 C, a chromosome balancer which carry the dominant larval marker *Tubby* (http://flybase.bio.

indiana.edu/); homozygous mutant larvae were recognized for their non-*Tubby* phenotype. All stocks were maintained on standard *Drosophila* medium at 25ºC.

Immunostaining of *Drosophila* neuroblast cells

Brains from third instar larvae were dissected and fixed according to Bonaccorsi et al. (2000). After two rinses in phosphate buffered saline (PBS), brain preparations were incubated overnight at 4°C with a monoclonal anti-a-tubulin antibody (Sigma), diluted 1:1000 in PBS and rabbit anti-Miranda antibody (a gift of Y. N. Jan) diluted 1:100 in PBS. After two rinses in PBS, primary antibodies were detected by 1 hour incubation at room temperature with FITC-conjugated anti-mouse IgG + IgM (1:20; Jackson Laboratories) and

Alexa-Fluor-555-conjugated anti-rabbit IgG (1:300; Molecular Probes), diluted in PBS. Immunostained preparations were mounted in Vectashield H-1200 (Vector Laboratories) containing DAPI (4,6 diamidino-2- phenylindole). The angle between a line connecting the two spindle poles and a line bisecting the crescent formed by Mira in metaphase NBs was measured, by hand with a goniometer, on images captured by a Zeiss Axioplan fluorescence microscope, equipped with an HBO100W mercury lamp and a cooled charged-coupled device (CCD camera; Photometrics CoolSnap HQ).

Microscopy

Imaging was performed using a Leica TCS SP5-AOBS 5-channel confocal system (Leica Microsystems) equipped with a 405nm diode, an argon ion and a 561nm DPSS laser. Fixed cells were imaged using a HCX PL APO 63x/1.4 NA oil immersion objective at a pixel resolution of 0.108 x 0.108 µm.

Time lapses were recorded overnight with an interval of 5 minutes using a 40X PlanApo N.A. 1.4 oil immersion objective on the cells kept in the microscope incubator at 37°C and 5% CO2.

Image analysis

Spindle angle measurements were obtained using a trigonometric formula, once measured the three dimensional (3D) distance (across the x, y, and z planes) and the 2D distance (across the z planes) between the two centrosomes of the spindle.

To quantify NuMA, Dynein and p150Glued signals at the centrosome, we used Fiji (fiji.sc; (Schindelin et al., 2012)). After obtaining the sum of intensity of all the Z stacks from multi stacks images, we built a ROI surrounding the signal at the centrosome and a ROI around the cells. Once the ROIs were established, they were used for all the images analyzed. We evaluated the Corrected Integrated Density (CTCF), for both the centrosomes, calculating as Integrated Density (Area of selection x Mean fluorescence of the background).

Measurement of astral-MT dynamics

Astral-MT nucleation frequencies were quantified as described (Samora et al., 2011) by counting the number of EB3 comets in the focal plane that originated from each spindle pole during the observation time. Cytoplasmic growth speeds for individual comets were measured as the total distance travelled from the spindle pole towards the cell cortex divided by the time. Kymographs of astral-MT and spindle-pole movements were obtained using Fiji.

Proximity Ligation Assay

PLA analysis (Soderberg et al., 2006) was performed using the kit provided by Olink Bioscience (Uppsala Science Park, Uppsala, Sweden). Metaphase HeLa cells and ASPM-GFP HeLa stable cell lines were incubated with the previously described primary antibodies and reactions were performed following manufacturer's instructions.

MT regrowth assay

48 h after siRNA transfection, MT were depolymerized at 4°C for 30 minutes. Cells were then washed and incubated in culture medium at 37°C to allow regrowth. Cells were fixed at different time intervals in methanol and processed for immunofluorescence microscopy to examine MT regrowth from spindle poles in metaphase cells. The MT signal was quantified using Fiji.

Centrosomal fractionation

Centrosome fractionation was performed as described previously (Reber, 2011). In brief, exponentially growing cells were incubated with 10 µg/ml nocodazole (Sigma-Aldrich) and 5 µg/ml Cytochalasin B (Sigma-Aldrich) for 90 min, and then lysed by hypotonic treatment. Centrosomes were harvested by centrifugation onto a 20% Ficoll cushion and further purified by centrifugation through a discontinuous (70, 50, and 40%) sucrose gradient. Fractions of 0.3 ml were collected and analyzed.

Western blotting

For immunoblots, equal amounts of proteins from whole-cell lysates were resolved by SDS–PAGE and blotted to nitrocellulose filters, which were then incubated with the indicated antibodies and developed using the ECL System (Amersham Biosciences).

Acknowledgements

We are grateful to Anne Straube (University of Warwick, Coventry, UK) for providing the EB3–tdTomato HeLa cell line, to Ina Poser and Antony Hyman (MPI, Dresden, Germany) for providing the GFP-BAC transgenic ASPM and CITK HeLa cell lines. This work was supported by the Telethon Foundation through grant n. GGP12095 to FDC.

Conflict of Interests

The authors declare that they have no conflict of interest.

Author contributions

All experiments were designed and conceived by M.G. and F.D.C. The mouse in vivo experiments were performed by F.T.B. with the support and the advice of W.B.H. The *Drosophila* experiments were performed by F.V. and S.B. The PLA experiment was performed by L.A. and A.S. The analysis of centrosome fractions were performed by A.B. and N.L. All the other experiments were performed by M.G, with the support of C.V., S.P., G.E.B., F.S. and A.A.C. ASPM reagents were provided by J.B. The manuscript was written by M.G. and F.D.C.

References

Ackman, J. B., Ramos, R. L., Sarkisian, M. R., and Loturco, J. J. (2007). Citron kinase is required for postnatal neurogenesis in the hippocampus. Dev Neurosci *29*, 113-123.

Arai, Y., Pulvers, J. N., Haffner, C., Schilling, B., Nusslein, I., Calegari, F., and Huttner, W. B. (2011). Neural stem and progenitor cells shorten S-phase on commitment to neuron production. Nat Commun *2*, 154.

Bassi, Z. I., Audusseau, M., Riparbelli, M. G., Callaini, G., and D'Avino, P. P. (2013). Citron kinase controls a molecular network required for midbody formation in cytokinesis. Proc Natl Acad Sci U S A *110*, 9782-9787.

Bassi, Z. I., Verbrugghe, K. J., Capalbo, L., Gregory, S., Montembault, E., Glover, D. M., and D'Avino, P. P. (2011). Sticky/Citron kinase maintains proper RhoA localization at the cleavage site during cytokinesis. J Cell Biol *195*, 595-603.

Bergstralh, D. T., and St Johnston, D. (2014). Spindle orientation: what if it goes wrong? Semin Cell Dev Biol *34*, 140-145.

Bettencourt-Dias, M., Hildebrandt, F., Pellman, D., Woods, G., and Godinho, S. A. (2011). Centrosomes and cilia in human disease. Trends Genet *27*, 307-315.

Bond, J., Roberts, E., Mochida, G. H., Hampshire, D. J., Scott, S., Askham, J. M., Springell, K., Mahadevan, M., Crow, Y. J., Markham, A. F.*, et al.* (2002). ASPM is a major determinant of cerebral cortical size. Nat Genet *32*, 316-320.

Busson, S., Dujardin, D., Moreau, A., Dompierre, J., and De Mey, J. R. (1998). Dynein and dynactin are localized to astral microtubules and at cortical sites in mitotic epithelial cells. Curr Biol *8*, 541-544.

Calegari, F., Haubensak, W., Haffner, C., and Huttner, W. B. (2005). Selective lengthening of the cell cycle in the neurogenic subpopulation of neural progenitor cells during mouse brain development. J Neurosci *25*, 6533-6538.

Calegari, F., and Huttner, W. B. (2003). An inhibition of cyclin-dependent kinases that lengthens, but does not arrest, neuroepithelial cell cycle induces premature neurogenesis. J Cell Sci *116*, 4947-4955.

Carminati, J. L., and Stearns, T. (1997). Microtubules orient the mitotic spindle in yeast through dynein-dependent interactions with the cell cortex. J Cell Biol *138*, 629-641.

Castanon, I., and Gonzalez-Gaitan, M. (2011). Oriented cell division in vertebrate embryogenesis. Curr Opin Cell Biol *23*, 697-704.

Chenn, A., and McConnell, S. K. (1995). Cleavage orientation and the asymmetric inheritance of Notch1 immunoreactivity in mammalian neurogenesis. Cell *82*, 631-641.

D'Avino, P. P., Savoian, M. S., and Glover, D. M. (2004). Mutations in sticky lead to defective organization of the contractile ring during cytokinesis and are enhanced by Rho and suppressed by Rac. J Cell Biol *166*, 61-71.

Di Cunto, F., Imarisio, S., Hirsch, E., Broccoli, V., Bulfone, A., Migheli, A., Atzori, C., Turco, E., Triolo, R., Dotto, G. P.*, et al.* (2000). Defective neurogenesis in citron kinase knockout mice by altered cytokinesis and massive apoptosis. Neuron *28*, 115-127.

Echard, A., Hickson, G. R., Foley, E., and O'Farrell, P. H. (2004). Terminal cytokinesis events uncovered after an RNAi screen. Curr Biol *14*, 1685-1693.

Faheem, M., Naseer, M. I., Rasool, M., Chaudhary, A. G., Kumosani, T. A., Ilyas, A. M., Pushparaj, P., Ahmed, F., Algahtani, H. A., Al-Qahtani, M. H., and Saleh Jamal, H. (2015). Molecular genetics of human primary microcephaly: an overview. BMC Med Genomics *8 Suppl 1*, S4.

Feng, Y., and Walsh, C. A. (2004). Mitotic spindle regulation by Nde1 controls cerebral cortical size. Neuron *44*, 279-293.

Fietz, S. A., and Huttner, W. B. (2011). Cortical progenitor expansion, self-renewal and neurogenesis-a polarized perspective. Curr Opin Neurobiol *21*, 23-35.

Fish, J. L., Kosodo, Y., Enard, W., Paabo, S., and Huttner, W. B. (2006). Aspm specifically maintains symmetric proliferative divisions of neuroepithelial cells. Proc Natl Acad Sci U S A *103*, 10438-10443.

Florio, M., and Huttner, W. B. (2014). Neural progenitors, neurogenesis and the evolution of the neocortex. Development *141*, 2182-2194.

Furuyashiki, T., Fujisawa, K., Fujita, A., Madaule, P., Uchino, S., Mishina, M., Bito, H., and Narumiya, S. (1999). Citron, a Rho-target, interacts with PSD-95/SAP-90 at glutamatergic synapses in the thalamus. J Neurosci *19*, 109-118.

Gai, M., Camera, P., Dema, A., Bianchi, F., Berto, G., Scarpa, E., Germena, G., and Di Cunto, F. (2011). Citron kinase controls abscission through RhoA and anillin. Mol Biol Cell *22*, 3768-3778.

Gillies, T. E., and Cabernard, C. (2011). Cell division orientation in animals. Curr Biol *21*, R599-609.

Gruber, R., Zhou, Z., Sukchev, M., Joerss, T., Frappart, P. O., and Wang, Z. Q. (2011). MCPH1 regulates the neuroprogenitor division mode by coupling the centrosomal cycle with mitotic entry through the Chk1-Cdc25 pathway. Nat Cell Biol *13*, 1325-1334.

Gruneberg, U., Neef, R., Li, X., Chan, E. H., Chalamalasetty, R. B., Nigg, E. A., and Barr, F. A. (2006). KIF14 and citron kinase act together to promote efficient cytokinesis. J Cell Biol *172*, 363-372.

Higgins, J., Midgley, C., Bergh, A. M., Bell, S. M., Askham, J. M., Roberts, E., Binns, R. K., Sharif, S. M., Bennett, C., Glover, D. M.*, et al.* (2010). Human ASPM participates in spindle organisation, spindle orientation and cytokinesis. BMC Cell Biol *11*, 85.

Homem, C. C., and Knoblich, J. A. (2012). Drosophila neuroblasts: a model for stem cell biology. Development *139*, 4297-4310.

Hutchins, J. R., Toyoda, Y., Hegemann, B., Poser, I., Heriche, J. K., Sykora, M. M., Augsburg, M., Hudecz, O., Buschhorn, B. A., Bulkescher, J.*, et al.* (2010). Systematic analysis of human protein complexes identifies chromosome segregation proteins. Science *328*, 593-599.

Kaindl, A. M., Passemard, S., Kumar, P., Kraemer, N., Issa, L., Zwirner, A., Gerard, B., Verloes, A., Mani, S., and Gressens, P. (2010). Many roads lead to primary autosomal recessive microcephaly. Prog Neurobiol *90*, 363-383.

Konno, D., Shioi, G., Shitamukai, A., Mori, A., Kiyonari, H., Miyata, T., and Matsuzaki, F. (2008). Neuroepithelial progenitors undergo LGN-dependent planar divisions to maintain self-renewability during mammalian neurogenesis. Nat Cell Biol *10*, 93-101.

Kosodo, Y., Roper, K., Haubensak, W., Marzesco, A. M., Corbeil, D., and Huttner, W. B. (2004). Asymmetric distribution of the apical plasma membrane during neurogenic divisions of mammalian neuroepithelial cells. Embo J *23*, 2314-2324.

Lancaster, M. A., and Knoblich, J. A. (2012). Spindle orientation in mammalian cerebral cortical development. Curr Opin Neurobiol *22*, 737-746.

Liu, H., Di Cunto, F., Imarisio, S., and Reid, L. M. (2003). Citron kinase is a cell cycle-dependent, nuclear protein required for G2/M transition of hepatocytes. J Biol Chem *278*, 2541-2548.

Loffler, H., Fechter, A., Matuszewska, M., Saffrich, R., Mistrik, M., Marhold, J., Hornung, C., Westermann, F., Bartek, J., and Kramer, A. (2011). Cep63 recruits Cdk1 to the centrosome: implications for regulation of mitotic entry, centrosome amplification, and genome maintenance. Cancer Res *71*, 2129-2139.

LoTurco, J. J., Sarkisian, M. R., Cosker, L., and Bai, J. (2003). Citron kinase is a regulator of mitosis and neurogenic cytokinesis in the neocortical ventricular zone. Cereb Cortex *13*, 588-591.

Madaule, P., Eda, M., Watanabe, N., Fujisawa, K., Matsuoka, T., Bito, H., Ishizaki, T., and Narumiya, S. (1998). Role of citron kinase as a target of the small GTPase Rho in cytokinesis. Nature *394*, 491-494.

Maliga, Z., Junqueira, M., Toyoda, Y., Ettinger, A., Mora-Bermudez, F., Klemm, R. W., Vasilj, A., Guhr, E., Ibarlucea-Benitez, I., Poser, I.*, et al.* (2013). A genomic toolkit to investigate kinesin and myosin motor function in cells. Nat Cell Biol *15*, 325-334.

Malik, R., Lenobel, R., Santamaria, A., Ries, A., Nigg, E. A., and Korner, R. (2009). Quantitative analysis of the human spindle phosphoproteome at distinct mitotic stages. J Proteome Res *8*, 4553-4563.

Matsumura, S., Hamasaki, M., Yamamoto, T., Ebisuya, M., Sato, M., Nishida, E., and Toyoshima, F. (2012). ABL1 regulates spindle orientation in adherent cells and mammalian skin. Nat Commun *3*, 626.

Megraw, T. L., Sharkey, J. T., and Nowakowski, R. S. (2011). Cdk5rap2 exposes the centrosomal root of microcephaly syndromes. Trends Cell Biol *21*, 470-480.

Mochida, G. H. (2009). Genetics and biology of microcephaly and lissencephaly. Semin Pediatr Neurol *16*, 120-126.

Mora-Bermudez, F., Matsuzaki, F., and Huttner, W. B. (2014). Specific polar subpopulations of astral microtubules control spindle orientation and symmetric neural stem cell division. Elife *3*.

Morin, X., and Bellaiche, Y. (2011). Mitotic spindle orientation in asymmetric and symmetric cell divisions during animal development. Dev Cell *21*, 102-119.

Naim, V., Imarisio, S., Di Cunto, F., Gatti, M., and Bonaccorsi, S. (2004). Drosophila citron kinase is required for the final steps of cytokinesis. Mol Biol Cell *15*, 5053-5063.

Neumann, B., Walter, T., Heriche, J. K., Bulkescher, J., Erfle, H., Conrad, C., Rogers, P., Poser, I., Held, M., Liebel, U.*, et al.* (2010). Phenotypic profiling of the human genome by time-lapse microscopy reveals cell division genes. Nature *464*, 721-727.

Nguyen-Ngoc, T., Afshar, K., and Gonczy, P. (2007). Coupling of cortical dynein and G alpha proteins mediates spindle positioning in Caenorhabditis elegans. Nat Cell Biol *9*, 1294-1302.

Noatynska, A., Gotta, M., and Meraldi, P. (2012). Mitotic spindle (DIS)orientation and DISease: cause or consequence? J Cell Biol *199*, 1025-1035.

Noctor, S. C., Martinez-Cerdeno, V., Ivic, L., and Kriegstein, A. R. (2004). Cortical neurons arise in symmetric and asymmetric division zones and migrate through specific phases. Nat Neurosci *7*, 136-144.

Nousiainen, M., Sillje, H. H., Sauer, G., Nigg, E. A., and Korner, R. (2006). Phosphoproteome analysis of the human mitotic spindle. Proc Natl Acad Sci U S A *103*, 5391-5396.

Panousopoulou, E., and Green, J. B. (2014). Spindle orientation processes in epithelial growth and organisation. Semin Cell Dev Biol *34*, 124-132.

Paramasivam, M., Chang, Y. J., and LoTurco, J. J. (2007). ASPM and citron kinase co-localize to the midbody ring during cytokinesis. Cell Cycle *6*, 1605-1612.

Paridaen, J. T., and Huttner, W. B. (2014). Neurogenesis during development of the vertebrate central nervous system. EMBO Rep *15*, 351-364.

Peyre, E., and Morin, X. (2012). An oblique view on the role of spindle orientation in vertebrate neurogenesis. Dev Growth Differ *54*, 287-305.

Pramparo, T., Youn, Y. H., Yingling, J., Hirotsune, S., and Wynshaw-Boris, A. (2010). Novel embryonic neuronal migration and proliferation defects in Dcx mutant mice are exacerbated by Lis1 reduction. J Neurosci *30*, 3002-3012.

Pulvers, J. N., Bryk, J., Fish, J. L., Wilsch-Brauninger, M., Arai, Y., Schreier, D., Naumann, R., Helppi, J., Habermann, B., Vogt, J.*, et al.* (2010). Mutations in mouse Aspm (abnormal spindle-like microcephaly associated) cause not only microcephaly but also major defects in the germline. Proc Natl Acad Sci U S A *107*, 16595-16600.

Reber, S. (2011). Isolation of centrosomes from cultured cells. Methods Mol Biol *777*, 107-116.

Samora, C. P., Mogessie, B., Conway, L., Ross, J. L., Straube, A., and McAinsh, A. D. (2011). MAP4 and CLASP1 operate as a safety mechanism to maintain a stable spindle position in mitosis. Nat Cell Biol *13*, 1040-1050.

Sarkisian, M. R., Li, W., Di Cunto, F., D'Mello, S. R., and LoTurco, J. J. (2002). Citron-kinase, a protein essential to cytokinesis in neuronal progenitors, is deleted in the flathead mutant rat. J Neurosci *22*, RC217.

Sauer, G., Korner, R., Hanisch, A., Ries, A., Nigg, E. A., and Sillje, H. H. (2005). Proteome analysis of the human mitotic spindle. Mol Cell Proteomics *4*, 35-43.

Saunders, R. D., Avides, M. C., Howard, T., Gonzalez, C., and Glover, D. M. (1997). The Drosophila gene abnormal spindle encodes a novel microtubule-associated protein that associates with the polar regions of the mitotic spindle. J Cell Biol *137*, 881-890.

Schindelin, J., Arganda-Carreras, I., Frise, E., Kaynig, V., Longair, M., Pietzsch, T., Preibisch, S., Rueden, C., Saalfeld, S., Schmid, B.*, et al.* (2012). Fiji: an open-source platform for biological-image analysis. Nat Methods *9*, 676-682.

Schwamborn, J. C., and Knoblich, J. A. (2008). LIS1 and spindle orientation in neuroepithelial cells. Cell Stem Cell *2*, 193-194.

Shandala, T., Gregory, S. L., Dalton, H. E., Smallhorn, M., and Saint, R. (2004). Citron kinase is an essential effector of the Pbl-activated Rho signalling pathway in Drosophila melanogaster. Development *131*, 5053-5063.

Sir, J. H., Barr, A. R., Nicholas, A. K., Carvalho, O. P., Khurshid, M., Sossick, A., Reichelt, S., D'Santos, C., Woods, C. G., and Gergely, F. (2011). A primary microcephaly protein complex forms a ring around parental centrioles. Nat Genet *43*, 1147-1153.

Soderberg, O., Gullberg, M., Jarvius, M., Ridderstrale, K., Leuchowius, K. J., Jarvius, J., Wester, K., Hydbring, P., Bahram, F., Larsson, L. G., and Landegren, U. (2006). Direct observation of individual endogenous protein complexes in situ by proximity ligation. Nat Methods *3*, 995-1000.

Straube, A., and Merdes, A. (2007). EB3 regulates microtubule dynamics at the cell cortex and is required for myoblast elongation and fusion. Curr Biol *17*, 1318-1325.

Taverna, E., Gotz, M., and Huttner, W. B. (2014). The cell biology of neurogenesis: toward an understanding of the development and evolution of the neocortex. Annu Rev Cell Dev Biol *30*, 465-502.

Thornton, G. K., and Woods, C. G. (2009). Primary microcephaly: do all roads lead to Rome? Trends Genet *25*, 501-510.

Wakefield, J. G., Bonaccorsi, S., and Gatti, M. (2001). The drosophila protein asp is involved in microtubule organization during spindle formation and cytokinesis. J Cell Biol *153*, 637-648.

Wandke, C., Barisic, M., Sigl, R., Rauch, V., Wolf, F., Amaro, A. C., Tan, C. H., Pereira, A. J., Kutay, U., Maiato, H.*, et al.* (2012). Human chromokinesins promote chromosome congression and spindle microtubule dynamics during mitosis. J Cell Biol *198*, 847-863.

Williams, S. E., and Fuchs, E. (2013). Oriented divisions, fate decisions. Curr Opin Cell Biol *25*, 749-758.

Yang, Y., Liu, M., Li, D., Ran, J., Gao, J., Suo, S., Sun, S. C., and Zhou, J. (2014). CYLD regulates spindle orientation by stabilizing astral microtubules and promoting dishevelled-NuMA-dynein/dynactin complex formation. Proc Natl Acad Sci U S A *111*, 2158-2163.

Yingling, J., Youn, Y. H., Darling, D., Toyo-Oka, K., Pramparo, T., Hirotsune, S., and Wynshaw-Boris, A. (2008). Neuroepithelial stem cell proliferation requires LIS1 for precise spindle orientation and symmetric division. Cell *132*, 474-486.

Figure legends

Figure 1. CITK controls mitotic spindle orientation.

(A) WT and CITK -/- embryonic (E14.5) mouse cerebral cortex were stained for α-tubulin (red) and DNA (blue). The ventricular plane is marked by a red dashed line, and the spindle axis of apical progenitors is indicated by a white dashed line. The angle between these two lines represents the mitotic angle.

(B) Quantification of vertical divisions of apical progenitors in WT and CITK -/- mice. n= 3 per each genotype.

(C) Quantification of cell cycle exit (ratio of cells BrdU+/Ki67− to all cells that incorporated BrdU) in the ventricular zone (VZ), subventricular zone (SVZ), intermediate zone (IZ) and

cortical plate (CP). Pregnant CITK +/- females, crossed with CITK +/- males, were injected with BrdU at E13.5; 24 hours later (E14.5) WT and CITK -/- embryonic mouse cerebral cortex were fixed in 4% PFA, cryosectioned and stained for Ki67 (green) and BrdU (red). n= 4 per each genotype.

(D) Neuroblasts of wild type and *ck* alleles immunostained for α-tubulin and Miranda. Note that whereas in wild type cells there is a tight coupling of the mitotic spindle with the polarity axis, in *ck* alleles the spindle show a more oblique orientation respect to Mira crescent.

(E) Distribution of spindle angle amplitude (°) in neuroblasts of wild type and *ck* alleles (n=58).

(F) Selected frames from time-lapse imaging experiments (see movies 1 and 2) showing two dividing cells transfected with either control (CTRL) or CITK siRNA, respectively. Note one of the two daughter cells in the lower panel (red arrow) going out of focus as a consequence of oblique division.

(G) Graphical representation of vertical and oblique divisions. The cleavage plane is indicated by a black dashed line.

(H) Quantification of oblique divisions of HeLa cells transfected with CTRL or CITK siRNA (n > 50 cells, 3 independent experiments).

(I) Control or CITK-depleted cells were immunostained for γ-tubulin (red) and DNA (blue) and imaged in z (0.3 μm-thick sections).). Upper panel: maximum intensity projections of confocal z-stacks are shown. Lower panel: cross-section (XZ) through the two poles of the same cell.

(J) Quantification and distribution of spindle angles (°) in control and in CITK-depleted cells. The values represent the angles between the axis crossing the two poles of metaphase spindles and the coverslip. (n ≥ 150 cells, 6 independent experiments).

Scale bars, 5μm. Data presented in (B), (C), (E), (H), and (J) are means ± SEM. Statistical significance was assessed using a two tails Student T-test. *** P < 0.001, ** P < 0.01; * P < 0.05.

Figure 2. CITK is associated with mitotic spindle poles through ASPM.

(A) HeLa cells pre-extracted for 1 min with 0.5% Triton X-100 in PHEM buffer and immunostained for CITK (green), γ-tubulin (red) and DNA (blue). Scale bars, 10μm

(B) HeLa cells expressing CITK-GFP from a BAC transgene treated as in (A) and immunostained for GFP (green), γ-tubulin (red) and DNA (blue). Scale bars, 5μm

(C) Western blot of centrosome-containing fractions from HeLa cells, showing that CITK co-purifies with γ‑tubulin.

(D) HeLa cells pre-extracted 1 min with 0.5% Triton X-100 in PHEM buffer and immunostained for CITK (green), ASPM (red) and DNA (blue).

(E) HeLa cells expressing CITK-GFP treated as in (A) and immunostained for GFP (green), ASPM (red) and DNA (blue).

(F) Close physical proximity between CITK with ASPM revealed by PLA on ASPM-GFP-expressing HeLa cells immunostained for GFP and CITK.

(G) Control or CITK-depleted cells immunostained for ASPM (green), γ-tubulin (red) and DNA (blue).

(H) Control or ASPM-depleted cells treated as in (A) and immunostained for CITK (green), γ-tubulin (red) and DNA (blue). Graph: Quantification of CITK positive centrosomes in control and ASPM-depleted cells. (n ≥ 75 cells, 4 independent experiments).

Data presented are means ± SEM. *** P < 0.001. All cell images represent maximum intensity projections of confocal z-stacks. Scale bars, 5μm if not specified otherwise.

Figure 3. CITK regulates astral MT and spindle orientation downstream of ASPM and through a kinase-dependent mechanism.

(A) Control, CITK or ASPM-depleted HeLa cells immunostained for α-tubulin (red) and DNA (blue). Maximum intensity projections of confocal z-stacks are shown.

(B) Quantification of astral MT number and maximal length in HeLa cells transfected with CTRL, CITK or ASPM siRNA (n > 130 cells, 3 independent experiments).

(C) Quantification of the rescue of astral MT number after CITK overexpression in ASPM-depleted HeLa cells (n > 50 cells, 2 independent experiments).

(D) Quantification of spindle orientation rescue after overexpression of CITK, CITN (lacking the kinase domain) or CKD (Citron kinase dead) mutants in ASPM-depleted HeLa cells (n > 50 cells, 3 independent experiments).

(E) Synchronized HeLa transfected with control, ASPM- or CITK-specific siRNAs treated with DMSO or with 250 pM Paclitaxel (taxol) 30 min before immunostaining for α-Tubulin. Spindle angles were measured as above (n > 100 cells, 6 independent experiments).

Data presented in (B), (C), (D) and (E) are means ± SEM. *** P < 0.001. All cell images represent maximum intensity projections of confocal z-stacks. Scale bars, 5μm.

Figure 4. Loss of CITK decreases astral MT length, stability and nucleation.

(A) Exemplar image of EB3–tdTomato HeLa cell used for kymograph analyses. To assess astral MT number and dynamics a line (blue) was added to images from the pole to the cortex.

(B) Kymographs of pole (bottom)-to-cortex (top) line scans of control and CITK-depleted EB3–tdTomato HeLa cells. The maximum projection of a 20-pixel-wide line (exemplified above) was plotted at 500 ms time intervals from left to right. MT growth results in diagonal lines.

(C) Quantification of astral MT dynamics. MT stability, length, growth speed (n > 250 MT, 30 cells) and nucleation frequency were calculated (n > 30 cells, 2 independent experiments).

(D) Immunofluorescence microscopy images showing MT regrowth at mitotic spindle poles 0, 5, 10 and 15 min after nocodazole washout. Control and CITK-depleted cells were immunostained for α-tubulin (red) and DNA (blue).

(E) Percentage of cells showing detectable MT nucleation (aster size > 1 μm) 0, 5, 10 and 15 min after nocodazole washout and quantification of aster size 15 min after nocodazole washout (n > 100 cells, 4 independent experiments).

In (C) and (E) data are presented as mean ± SEM. Student's t test value **, $P < 0.01$; ***, $P < 0.001$. Scale bar, 5 μm.

Movies 1 and 2. CITK depletion induces abnormal spindle orientation.

Mitotic spindles of control (Movie 1) or CITK RNAi-treated (Movie 2) HeLa cells were analyzed by time-lapse microscopy. Frames were taken every 5 min for 12 h.

Movie 3. CITK localization during cell division.

HeLa cells expressing physiological levels of GFP-CITK from a stably integrated BAC transgene were analyzed by time-lapse microscopy. Frames were taken every 5 min for 12h.

Figure 1

Gai M. et al.

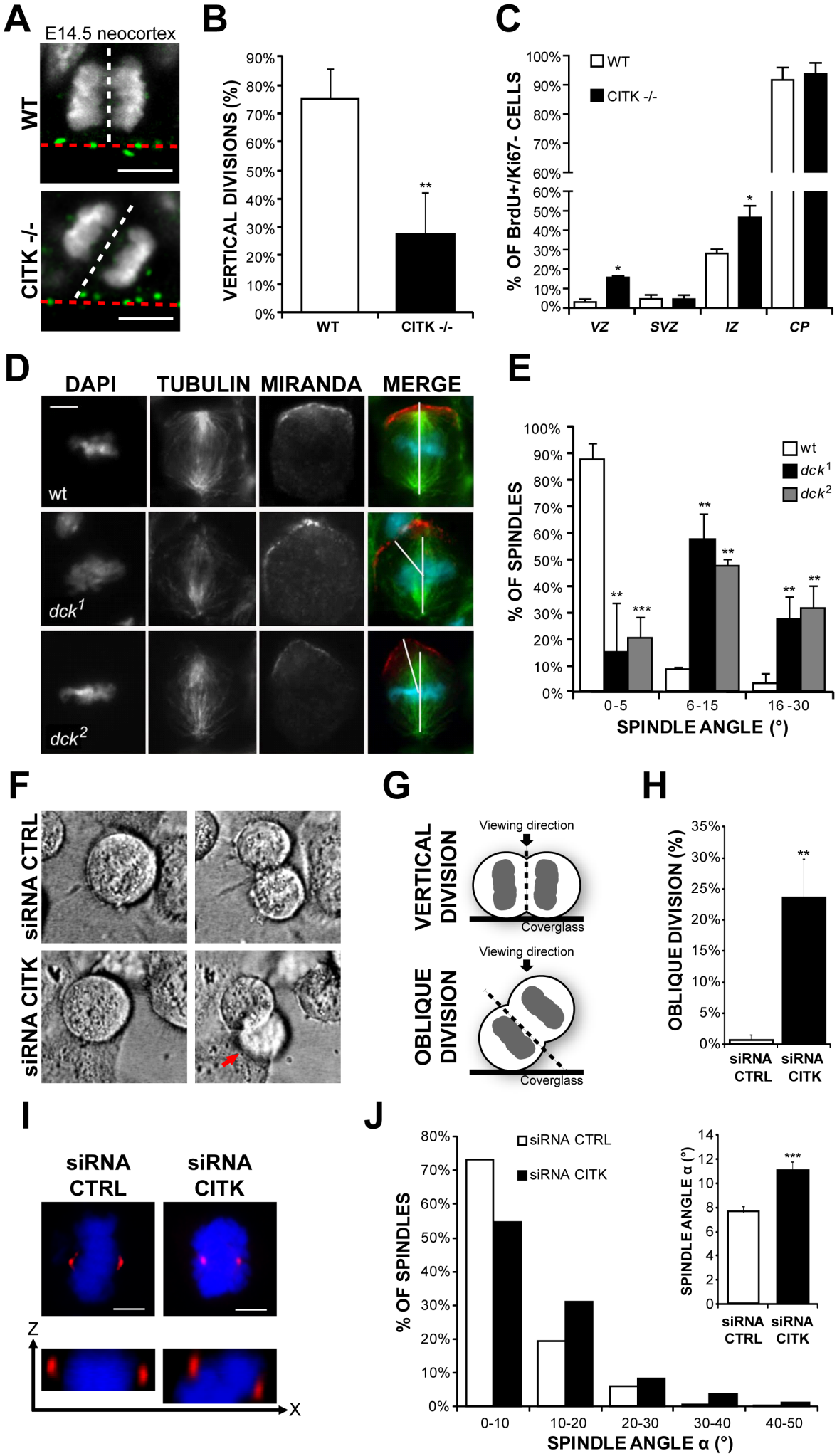

Figure 2

Gai M. et al.

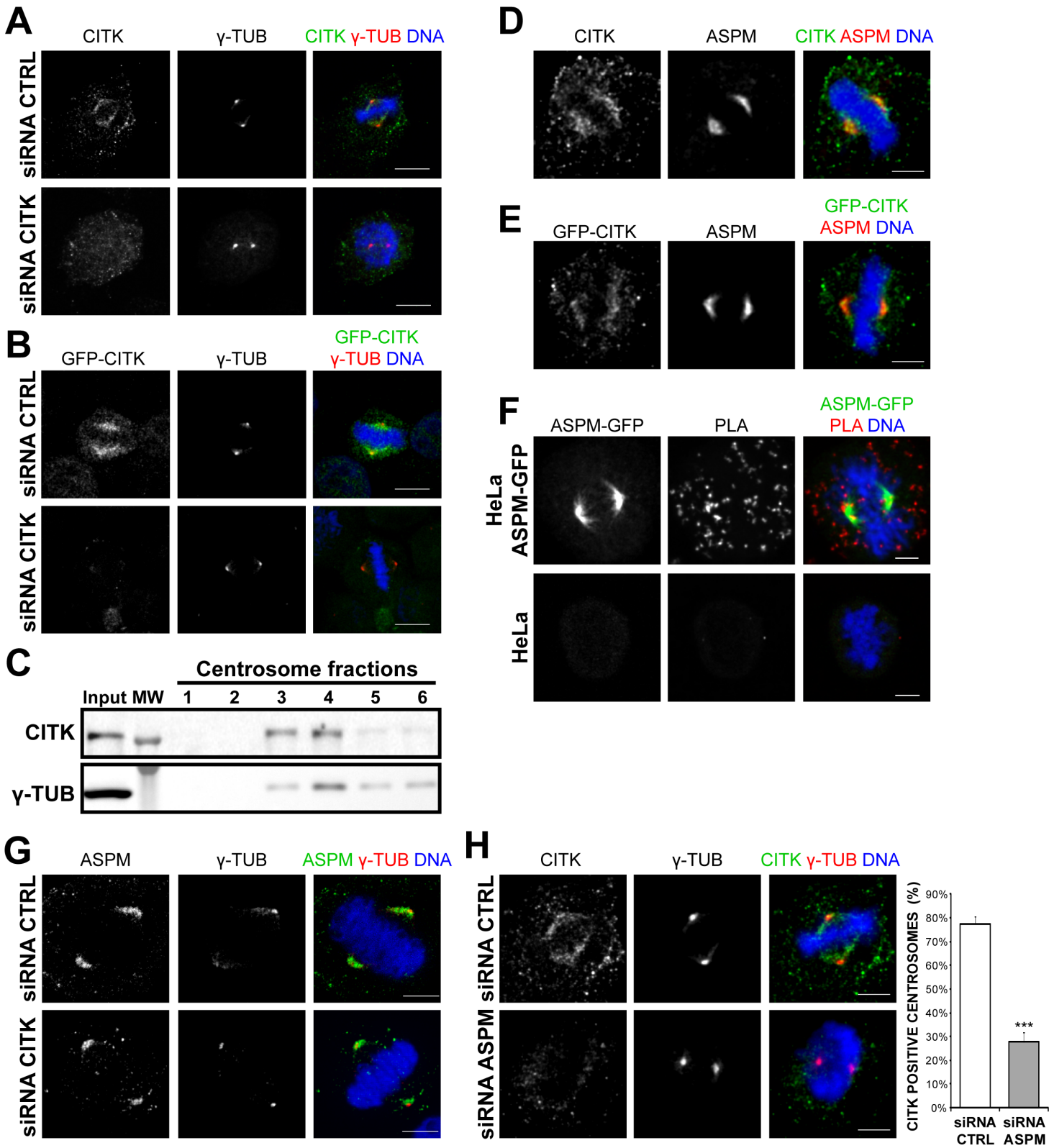

Figure 3

Gai M. et al.

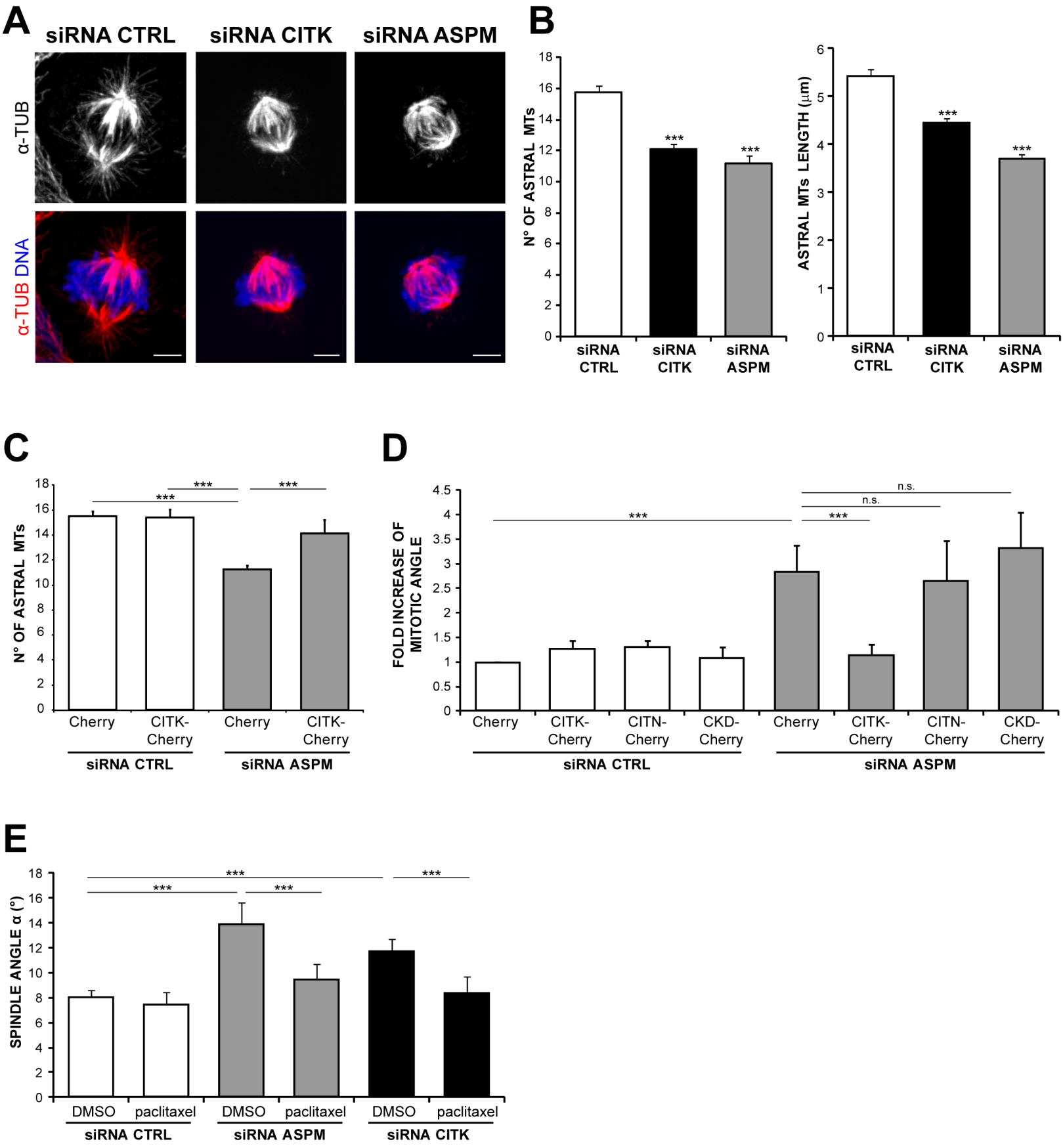

Figure 4

Gai M. et al.